Proceedings of Ninth World Conference on Earthquake Engineering
August 2-9, 1988, Tokyo-Kyoto, JAPAN (Vol.VIII)

SE-10

ACTIVE ISOLATION OF SENSITIVE EQUIPMENT FOR WEAK EARTHQUAKES

Takafumi FUJITA[1], Qing FENG[2], Eiji TAKENAKA[3],
Tetsuo TAKANO[4] and Yoji SUIZU[5]

[1]Associate Prof., Inst. of Industr. Sci., Univ. of Tokyo, Japan
[2]Graduate Student, Inst. of Industr. Sci., Univ. of Tokyo, Japan
[3]Ricoh Co., Ltd., Japan
[4]Mitsubishi Steel Mfg. Co., Ltd., Japan
[5]Bridgestone Co., Ltd., Japan

SUMMARY

In Japan seismic isolation of sensitive equipment is often required to prevent the yield rate of products from decreasing due to weak but frequent earthquakes. The isolation of monocrystal pullers is a typical example. The passive isolation devices used now sometimes fail to protect the monocrystals from earthquakes. Therefore an active isolation device with electric-hydraulic actuators was developed. The control system was designed by using the pole assignment method. Excitation tests showed that excellent reduction in the acceleration of the equipment mounted on the device could be achieved by the active isolation.

INTRODUCTION

In Japan seismic isolation has become increasingly necessary with the growing dominance of so-called "high technology" industries and is now being used to provide effective seismic protection for precision equipment which is of major importance in the industries (Ref.1). In such industrial facilities seismic isolation is often required to prevent the yield rate of complete products from decreasing due to weak but frequent earthquakes, rather than to protect the equipment itself from strong earthquakes. Seismic isolation of monocrystal pullers producing monocrystals for semiconductor devices, is a typical exampel of the use to improve productivity. The monocrystals have the shape of a solid cylinder with a very thin neck with a diameter of less than 5 mm at an end as shown in Fig.1. In the equipment, such a monocrystal is suspended by the very thin neck and grows longitudinally as it is pulled up very slowly from the molten material in a melting pot. The neck is easily broken even by weak earthquakes such as occur several times a year in Japan.

The passive isolation devices (Ref.2,3) are used now to prevent the suspended monocrystal from falling due to such earthquakes. The isolation devices are expected to have the performance to reduce the horizontal response acceleration of the equipment to 1/7—1/4 of that when non-isolated(Ref.2). The number of implementation is increasing year by year since the first implementation in 1984. The effectiveness of the isolation devices has already been demonstrated in real applications. In some cases, however, the isolation devices failed to protect the monocrystals. This is the reason why an active isolation device is required.

In this paper, studies of an active isolation device using electric-hydraulic actuators are described. This work is the first step in the development. The final object of the development is an active-passive isolation device which can provide active isolation for weak earthquakes and passive isolation for strong earthquakes.

ACTIVE ISOLATION DEVICE AND ITS ANALYTICAL MODEL

An Active Isolation Device Using Electric-Hydraulic Actuators The active isolation device developed for two-dimensional horizontal isolation has a structure shown schematically in cross-section in Fig.2. In this device, two pairs of linear motion elements crossing at right angles ensure that the table on which the equipment is mounted moves in horizontal translation without rotation. The isolation device is equipped in each direction with an electric-hydraulic actuator to exert control force on the table. In this study, however, a test model for one-dimensional active isolation was used (Fig.3). An equipment model was mounted on the table of the isolation device, and the table was controlled by the actuator to reduce the response acceleration of the equipment model.

Fig.1 A completed Monocrystal of Silicon being taken out

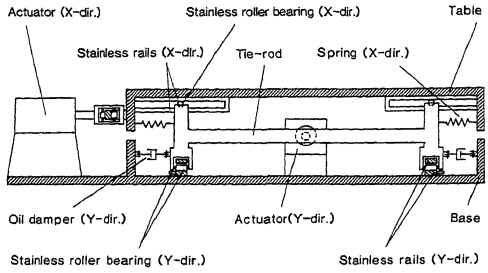

Fig.2 Structure of an Active Isolation Device

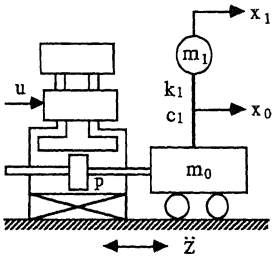

Fig.4 Analytical Model

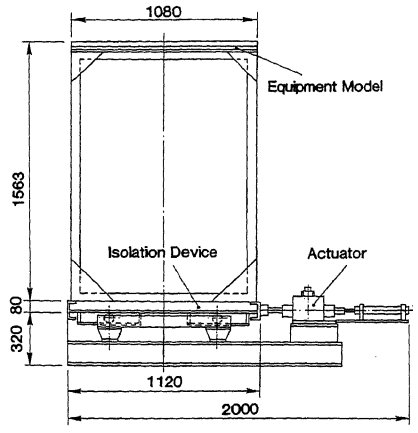

Fig.3 Experimental Model

Equations of Motion The analytical model shown in Fig.4 is considered for the experimental model. The equations of motion for this system are derived as follows.

$$\ddot{x}_1+2\zeta_1\omega_1(\dot{x}_1-\dot{x}_0)+\omega_1^2(x_1-x_0) = -\ddot{z} \quad (1)$$

$$\ddot{x}_0+\frac{\rho(2\zeta_1\omega_1)}{1-\rho}(\dot{x}_0-\dot{x}_1)+\frac{\rho\omega_1^2}{1-\rho}(x_0-x_1)+\frac{\mu g}{1-\rho}sgn(\dot{x}_0) = -\ddot{z}+\frac{\gamma}{1-\rho}p \quad (2)$$

$$r\dot{p}+lp+a\dot{x}_0 = bu-\frac{b|u|p}{2p_s} \quad (3)$$

where,

$$\frac{c_1}{m_1}=2\zeta_1\omega_1, \qquad \frac{k_1}{m_1}=\omega_1^2, \qquad \frac{m_1}{m_0+m_1}=\rho, \qquad \frac{a}{m_0+m_1}=\gamma,$$

x_0 : relative displacement of the isolation device to the floor (m)
x_1 : relative displacement of the equipment model to the floor (m)
$\ddot{z}$: earthquake acceleration of the floor (m/s²)
m_0 : mass of the isolation device (kg)
m_1 : mass of the equipment model (kg)
k_1 : spring constant of the equipment model (N/m)
c_1 : damping coefficient of the equipment (N·s/m)
μ : friction coefficient
p : hydraulic pressure (Pa)
p_s : pumping pressure (Pa)
u : input current of the servo valve (A)
q : output flow rate of the servo valve (m³/s)
b : flow gain of the servo valve (m³/s·A)
l : decreasing rate of output flow in the servo valve with increasing of load pressure or the decreasing rate of output flow by leakage inside the servo valve (m⁴·s/kg)
r : rigidity coefficient of the electric-hydraulic system (m⁴·s²/kg)
a : cross section of the cylinder (m²)

Parameter Identification In order to determine the unknown values of the above parameters, identification experiments were carried out, giving sinusoidal inputs to the servo valve. Moreover, in order to prevent the device from drift in displacement, a signal of the displacement was proportionally feedbacked into the input current. Therefore the input current is written as follows:

$$u = A\sin 2\pi ft - K_0x_0$$

where A is the amplitude of the sine input, f is the frequency of the input. K_0 was set to be 0.016A/m so that the displacement drift became as small as possible and the response became as fast as possible at the same time.

On the other hand, computer simulations were carried out according to Eq.(1)-(3). To make the accelerations of the equipment model and the device identical to the corresponding results of the above experiments, the values of the parameters were determined as follows.

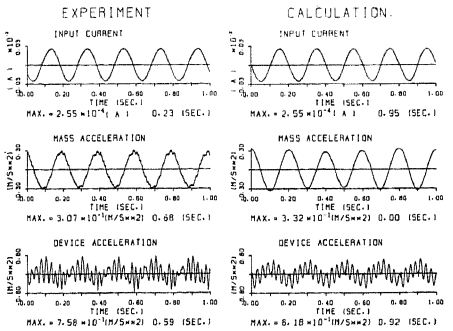

Fig.5 An Example of Identification

Table 1. Identified parameters

r	6.1*10⁻¹⁴	m⁴·s²/kg	m_0	2.48*10²	kg
l	6.8*10⁻¹³	m⁴·s/kg	m_1	5.54*10²	kg
b	2.6*10⁻²	m³/s·A	f_1	3.78	Hz
a	8.7*10⁻⁴	m²	ζ_1	1.0*10⁻²	
			μ	5.0*10⁻³	

Examples of the simulated and experimental results are shown in Fig.5. Fairly good agreement is obtained between these results.

DESIGN OF THE CONTROL SYSTEM

State Equations and Output Equations Through the simulation for the parameter identification mentioned above, it was also found that the nonlinear term of the Eq.(3) could be ignored because the distortion of the acceleration waves in Fig.5 was mainly caused by the nonlinearity of the friction. Hence, Eq.(3) can be simplified as,

$$r\dot{p}+lp+a\dot{x}_0 = b(u - K_0x_0) \tag{4}$$

Furthermore, replacing the friction term $\mu(m_0+m_1)g\cdot sgn(\dot{x}_0)$ with equivalent damp $c_e\dot{x}_0$, linearized state equations can be obtained as follows.

$$\dot{x}= Ax+Bu+D\ddot{z} \tag{5}$$

where,

$$x = [\ x_1 \quad \dot{x}_1 \quad x_0 \quad \dot{x}_0 \quad p]^{T}$$

$$A = \begin{bmatrix} 0 & 1 & 0 & 0 & 0 \\ -\omega_1^2 & -2\zeta_1\omega_1 & \omega_1^2 & 2\zeta_1\omega_1 & 0 \\ 0 & 0 & 0 & 1 & 0 \\ \frac{\rho\omega_1^2}{1-\rho} & \frac{\rho 2\zeta_1\omega_1}{1-\rho} & -\frac{\rho\omega_1^2}{1-\rho} & -\frac{\rho 2\zeta_1\omega_1}{1-\rho} - \frac{c_e}{m_0} & \frac{\gamma}{1-\rho} \\ 0 & 0 & -\frac{bK_0}{r} & -\frac{a}{r} & -\frac{l}{r} \end{bmatrix} \quad B= \begin{bmatrix} 0 \\ 0 \\ 0 \\ 0 \\ \frac{b}{r} \end{bmatrix} \quad D= \begin{bmatrix} 0 \\ -1 \\ 0 \\ -1 \\ 0 \end{bmatrix}$$

The absolute acceleration and the relative displacement of the equipment model $\ddot{x}_1+\ddot{z}$, x_1, the absolute acceleration and the relative displacement of the device $\ddot{x}_0+\ddot{z}$, x_0 and the driving force of the actuator ap were detected by sensors. Therefore, the output equations are given as follows.

$$y= Cx \tag{6}$$

where,

$$y = \begin{bmatrix} \ddot{x}_1+\ddot{z} \\ x_1 \\ \ddot{x}_0+\ddot{z} \\ x_0 \\ ap \end{bmatrix} \qquad C = \begin{bmatrix} -\omega_1^2 & -2\zeta_1\omega_1 & \omega_1^2 & -2\zeta_1\omega_1 & 0 \\ 1 & 0 & 0 & 0 & 0 \\ \frac{\rho\omega_1^2}{1-\rho} & \frac{\rho 2\zeta_1\omega_1}{1-\rho} & -\frac{\rho\omega_1^2}{1-\rho} & -\frac{\rho 2\zeta_1\omega_1}{1-\rho} - \frac{c_e}{m_0} & \frac{\gamma}{1-\rho} \\ 0 & 0 & 1 & 0 & 0 \\ 0 & 0 & 0 & 0 & a \end{bmatrix}$$

Design Method of the Control System The pole assignment method was applied to design the control system.

It is well known, if a system is controllable, the closed loop poles of feedback control can be arbitrarily assigned through state feedback $u = Kx$. In this design, the poles of the system were assigned to proper places to increase the period of the device which was effective for the isolation.

Hardware and Software of the Control System The control system is shown in Fig.6. The controller was a 16bit microcomputer (i8086) with a numerical coprocessor (i8087) to enable fast computation. The output signals detected by the sensors were sent to the microcomputer through 12bit A/D converters. Then the control input was calculated according to the method described above, and applied to the servo amplifier through 12bit D/A converter.

The computer control program was written in C language. As shown in the

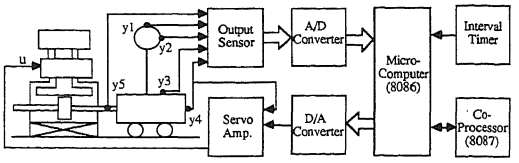

Fig.6 Control System

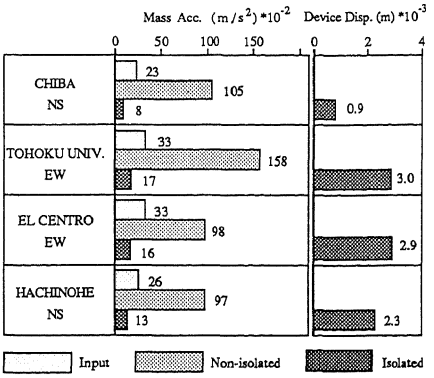

Fig.8 Performance of the Active Isolation Device

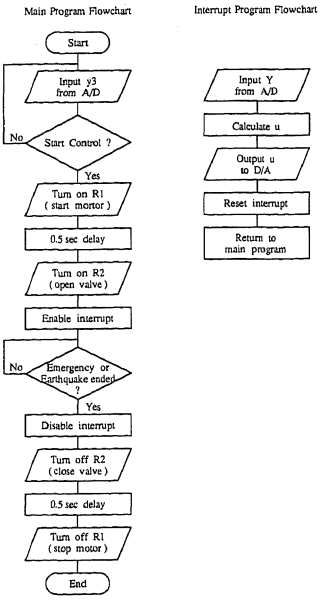

Fig.7 Flowchart of the Control Program

flowchart of Fig.7, when an earthquake is detected by the acceleration sensor attached to the isolation device, the microcomputer turns on the relays to start the motor and to open the valve, and then starts the control routine. The sampling time is 5msec. This is accomplished by sending an interrupt signal every 5msec to the CPU from a timer inside the computer. When the earthquake ends, the valve and the motor are turned off as the same way as they are started. Therefore, the active earthquake isolation can be automatically carried out.

EXPERIMENTAL RESULTS

Control Parameters The active isolation experiments were carried out with the following control parameters designed by the pole assignment method.

$$K = [\,1.21 \quad -1.64*10^{-5} \quad -1.21 \quad 3.88*10^{-5} \quad -5.67*10^{-11}\,] \tag{8}$$

The poles of the control system were assigned as shown in Table 2.

Table 2 Poles of the Control System

Open Loop	-0.4 ± j23.4	-6.5 ± j227	-0.49
Closed Loop	-18.5± j13.8	-0.43± j227	-0.49

Experimental Results In the excitation tests, various strong earthquake inputs were used including ground motion records from HACHINOHE, EL CENTRO, etc. as well as weak earthquake inputs such as CHIBA. In order to examine the isolation performance of the device in weak earthquakes, the peak accelerations of the strong earthquake inputs were decreased until 0.3 m/s².

Examples of the results are shown in Fig.8. For each test, the response accelerations of the equipment model when isolated and non-isolated to the same input are compared. Response displacements of the isolation device are also shown. These results show that the active device has the isolation performance to reduce the response acceleration of the equipment to 1/13— 1/6 of that when non-isolated. Fig.9 shows the responses to the EL CENTRO input when isolated and non-isolated.

A whole process of the active isolation for the CHIBA input is shown in Fig.10. It was confirmed that when a earthquake occured, the control system started immediately, and when the earthquake was over, it ended automatically.

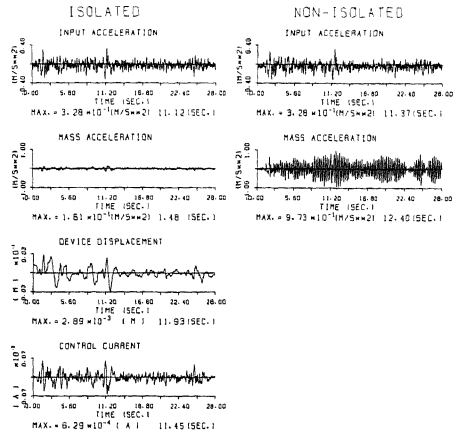

Fig.9 An Example of Time Histories of the Responses

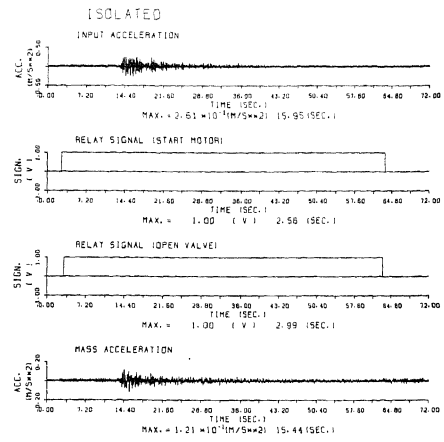

Fig.10 An Example of Time Histories of the Whole Processs

CONCLUDING REMARKS

An active isolation device using electric-hydraulic actuators has been developed. By actively controlling the device, the response acceleration of the equipment could be extremely reduced. However, comparing with the passive isolation, the isolation performance was not so superior as to be satisfactory.

The next steps in the research are considered as follows. 1)improving the distortion in the accelerations due to the friction, or replacing the actuator with a linear motor; 2)applying an observer to the control system to reduce the number of sensors; 3)developing an active-passive isolation device for both of weak earthquakes and strong earthquakes.

REFERENCES

1. Fujita, T., "Earthquake Isolation Technology for Industrial Facilities – Research, Development and Application in Japan", Bulletin of the New Zealand National Society for Earthquake Engineering, Vol. 18, No.3, (1985).
2. Fujita, T., Yogo, K., Omi, T. and Koizumi, T., "An Earthquake Isolation Device Using Linear Motion Mechanism", Trans. of the Japan Society of Mechanical Engineers, Vol. 50, No. 456, Ser. C, (in Japanese) (1984).
3. Fujita, T., Kuramoto, S. and Omi, T., "A Three-Dimensional Earthquake Isolation Device", Trans. of the Japan Society Mechanical Engineers, Vol.51, No.471, Ser. C, (in Japanese) (1985).